

Dynamic Compressive Response of Renal Cortex

Farhana Pervin^{1*}, Weinong W. Chen¹ and Tusit Weerasooriya²

¹*Schools of Aeronautics/Astronautics and Materials Engineering
Purdue University, West Lafayette, IN 47907, USA*

²*U.S. Army Research Laboratory, Aberdeen Proving Ground, MD 21005, USA*

Abstract

The compressive mechanical responses of bovine kidney tissues are characterized over a wide range of strain rates in this research. The specimens are taken from the cortex of fresh kidneys. A hydraulic materials testing system is used to conduct compression experiments at the quasi-static strain-rates of 0.01 s^{-1} and 0.1 s^{-1} as well as at the intermediate strain rates of 1 s^{-1} , 10 s^{-1} and 100 s^{-1} . A modified Kolsky compression bar is used to conduct experiments at higher strain-rates ranging from $1,000 \text{ s}^{-1}$ to $3,000 \text{ s}^{-1}$. The specimen geometry in high-rate experiments is also controlled to minimize inertia effects. The kidney tissues are characterized at every decade of strain rate over a five-decade range. The experiment results show that the non-linear compressive stress-strain behavior of the bovine renal cortex is highly sensitive to strain rates. The tissue stiffens significantly with increasing strain-rates.

Keywords: Kolsky bar, mechanical response, kidney tissue, strain-rate effect

1. Introduction

Renal injury is the most common urologic system injury and occurs in 8-10% of patients with abdominal injury. Renal injuries can be separated into blunt or penetrating injuries and results from a variety of mechanism. In the United States, traffic accidents are the most common cause of blunt abdominal injury. Blunt injury accounts for ~80% of renal injuries. Penetrating injury is less common (Baverstock et al., 2001). The renal injuries have been significantly reduced by improving the car safety measures. Despite the improvements in car safety designs during last few decades, much more remains to be done in accident and injury prevention (Rutledge et al., 1991). To further improve injury prevention methods, a better understanding of the underlying causes of renal injury is needed, which may lead to the effective design of new and more adequate protection measures.

Numerical simulation has become a powerful tool to reveal the detailed deformation processes under impact loading, especially in subjects that are not suitable for extensive instrumentation, such as soft tissues. For example, Schmidlin et al. (1996) studied the injury mechanism of renal trauma with a two-dimensional FEM (finite element method) model of the kidney. Their results suggest that the injury is caused by the combined effect of impact force and the reaction developed by the inner compartments filled with liquid. Examples like this and many others indicate that these engineering tools can become efficient diagnostic methods to predict body injuries caused by mechanical impact. However, realistic simulations require accurate material models that represent the material deformation and failure are incorporated in the simulation codes. Therefore, dynamic mechanical behaviors of biological tissues at various strain rates are needed as input data for the modeling and simulation, which will lead to improved diagnosis, surgical simulations and personnel training. In this research, our focus is on kidney tissues.

Kidney tissues have been characterized mechanically in simple shear under constant strain rate, stress relaxation, strain ramp and oscillatory loading (Nasseri et al., 2002). Experiments have also been conducted under compression and tension (Farhad et al., 1999), and aspiration (Nava et al., 2004). Farshad et al. (1999) conducted compression, tension and shear experiments on fresh pig kidney. Their study revealed that the uniaxial compression tests on the radial and tangential specimens from the cortex under various loading rates show an increase in the rupture stress with the increase in the loading rate and a decrease in the corresponding strain. Nasseri et al. (2002) investigated

*Email: fpervin@purdue.edu

the viscoelastic properties of pig kidney in shear. They characterized the cortex tissue under the loading conditions of oscillatory strain sweep, frequency sweep, stress relaxation and constant-rate shear. A material model was developed and fitted to their experimental data with a single set of parameters. Nava et al. (2004) characterized the mechanical behavior of human liver and kidney through in vivo aspiration experiments.

Different type of experiments discussed above is aimed at revealing different properties of the kidney tissue. In contrast, under impact loading conditions, no standard testing procedure exists for characterizing the dynamic response of soft tissues such as from the kidney. Furthermore, little data is available on the high strain rate behavior of kidney tissue. More experimental data for soft tissues are needed at high strain rate loading conditions to obtain material models that represent the dynamic behavior of tissues. The lack of documented data is partially due to the technical challenges associated with conducting high rate experiments on soft tissues. Pervin and Chen (2009) used a novel technique to experimentally determine the compressive behavior of brain tissues at high strain rates. This experimental technique was adopted to conduct experiments on kidney tissues reported in this paper.

In this study, we used a modified Kolsky bar to obtain compressive stress-strain response of kidney tissues at three high strain rates ($1,000\text{s}^{-1}$, $2,000\text{ s}^{-1}$ and $3,000\text{ s}^{-1}$). In order to determine the strain-rate effects of the bovine kidney tissues over a wider strain-rate range, we also conducted compression experiments at intermediate and quasi-static strain rates using a hydraulically driven material testing system (MTS810). In these experiments, the MTS machine was set to the mode of displacement control at five speeds, corresponding to the strain rates of 100 s^{-1} , 10 s^{-1} , 1 s^{-1} , 10^{-1} s^{-1} and 10^{-2} s^{-1} . Using these different test methods, the compressive stress-strain responses of the kidney tissues were obtained over a strain rate range of five decades, with data in every decade.

2. Experimental Techniques

At quasi-static and intermediate strain rates, we used a conventional MTS machine. The test-section configuration is identical to that was used in the Kolsky bar high-rate setup, such that the only variable in all different strain rate experiments is the strain rate. A load cell with $\pm 25\text{ lb}$ (111.2 N) capacity was used to record the axial load in quasi-static experiments. A piezoelectric load transducer with a 50 lb (222.41 N) capacity was used for intermediate rate experiments. The switch in load cells was necessary because a conventional load cell does not have a frequency response high enough for the intermediate-rate experiments. A thin layer of vegetable oil was applied to the surfaces of upper and lower platens to minimize friction. The stress and strain are measured as nominal values, which are defined as the force divided by the un-deformed cross-sectional area and the deformation divided by the un-deformed specimen thickness, respectively.

Kolsky bar, also known as split Hopkinson pressure bar (SHPB), has been widely used in characterizing the high-rate behavior of engineering materials (Gray, 2000). A conventional Kolsky bar consists of a striker bar, an incident bar, and a transmission bar. A specimen is placed between the incident and transmission bars. When the striker bar impacts the incident bar, an elastic compressive stress pulse, referred to as the incident pulse, is generated and propagates along the incident bar to the specimen. When the incident pulse reaches the specimen, part of the pulse is reflected backward into the incident bar due to the impedance mismatch at the bar-specimen interface, and the remaining part of the pulse is transmitted into the specimen, and eventually, into the transmission bar. Axial strain gages mounted on the surfaces of the incident and transmission bars provide time-resolved measures of the elastic strain pulses in the bars. We have modified the Kolsky bar to accurately determine the dynamic response of soft tissues. Due to the low mechanical impedance of the specimen, the transmitted signal has very small amplitude. In order to increase the amplitude of the transmitted signal, a hollow aluminum transmission bar with semiconductor strain gage was used (Chen et al., 1998). Quartz-crystals were installed on both sides of the soft specimen to verify dynamic equilibrium across the specimen (Chen et al., 2000; Casem et al., 2005). A pulse-shaping technique (Frew et al., 2002) was used to control the profile of the loading pulse to ensure dynamic stress equilibrium across the soft specimen. The controlled pulse also facilitates the dynamic deformation at constant strain rates.

A schematic of the Kolsky bar used in this study is shown in Figure 1. The 7075-T6 aluminum incident bar is 19 mm in diameter and 3658 mm in length. A 2438-mm long aluminum (7075-T6) tube of 19 mm in outer diameter and 1.5 mm in wall thickness was used as the transmission bar. The incident and reflected signals were measured by a pair of resistive strain gages mounted in the middle of the incident bar. The transmitted signal was detected from the semiconductor strain gages mounted on the transmission bar. When the specimen deforms under dynamic stress equilibrium,

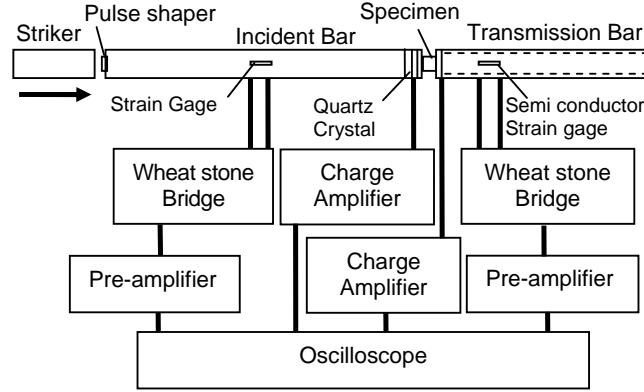


Figure 1: A schematic of a Kolsky bar modified for experiments on soft tissues.

the strain rate, strain and stress histories in the specimen can be calculated by using the following equations, respectively (Chen et al., 1998).

$$\dot{\varepsilon} = \frac{C_0}{L_s} \left[\left(1 - \frac{A_t}{A_i} \right) \varepsilon_i(t) - \left(1 + \frac{A_t}{A_i} \right) \varepsilon_r(t) \right] \quad (1)$$

$$\varepsilon = \int_0^t \dot{\varepsilon}(\tau) d\tau \quad (2)$$

$$\sigma = \frac{A_t}{A_s} E_0 \varepsilon_i(t) \quad (3)$$

where $\varepsilon_i(t)$ and $\varepsilon_r(t)$ are the time-resolved incident and transmitted strains in the incident and transmission bars of cross-sectional area A_i and A_t , respectively; E_0 is Young's modulus of the bar material; A_s is the initial cross-sectional area of the specimen; L_s is the original length of the specimen; $\varepsilon_r(t)$ is the reflected strain in the incident bar; and C_0 is the elastic bar wave speed in the bar material. The foregoing calculations assume that the elastic bars are made of the same material.

3. Specimen Preparation

The experiments were performed *in vitro* on specimens taken from a fresh bovine kidney. The kidneys of an 18 months old steers were collected from a slaughter house of animal science department of Purdue University, a few minutes after sacrifice. The kidneys were taken as a by-product of the meat. To prevent fast degradation of the kidneys, they were preserved in kreb solution at room temperature. All the experiments were completed within six hours postmortem. As shown in Figure 2, cylindrical samples were cut perpendicular to the blood vein direction (D1) and parallel (D2) to the vein directions in the cortex. Trepchine blades with very sharp edges were used to harvest the cylinders with a diameter of 10 mm. These cylinders were then sliced to disks of 1.7 mm in thickness by a scalpel with the help of a 1.7 mm thickness gage. Finally, a 5 mm diameter hole was cut through the specimen center by a sharp punch. The specimen dimensions are also shown in Figure 2. The initial specimen diameter (± 1 mm) and thickness (± 0.1 mm) were measured with dial calipers. A thin hollow disc specimen was used to minimize the inertia effects (Song et al., 2007). It was observed that the specimens remained fresh and no swelling was observed during the sample preparation and testing. Each specimen was prepared just before the mechanical loading. Kidney tissue is very soft and sticky. It was challenging to obtain an exact cylindrical shape. A thickness gage was used to obtain exact thickness. The specimen's cross-sectional geometry was printed on the loading surfaces to ensure consistently shaped specimens were installed on the loading surfaces prior to mechanical loading.

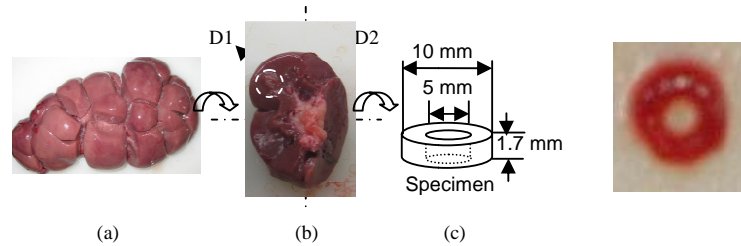


Figure 2: Illustration of kidney tissue specimen preparation: (a) Bovine kidney. (b) Harvesting cylindrical specimens. (c) Specimen geometry

Biological tissues are not ideal for traditional type of mechanical testing. There are variations of the structure of the material and properties from specimen to specimen. In order to determine the trends in mechanical response from statistically analysis, experiments were conducted on fifteen kidney tissue specimens at each strain rate. Three different bovine kidneys were used for each strain rate and a minimum of five specimens was used from each kidney ($n=3 \times 5$). Each specimen was tested once only. Due to its more uniform texture, only the renal cortex was used in this study. The thickness of renal cortex is only a few millimeters. The specimens were taken from different lobes to obtain tissues of sufficient sizes for the specimens.

4. Experimental Results and Discussions

Figure 3 shows the experimental results obtained from uniaxial compression tests conducted at quasi-static and intermediate strain rates. The stress-strain curve represents the average of fifteen experiments for each strain rate. The results shown in Figure 3 reveal that the kidney tissues exhibit non-linear stress-strain behavior. The tissues responses stiffen up with increasing loading rates, suggesting the rate dependency of the tissue. These results are obtained at strain rates below 100 s^{-1} , and are seen consistent with the results reported by Farshad et al. (1999) at strain rates of 0.16 s^{-1} and 0.016 s^{-1} .

From Kolsky bar high-rate experiments, Figure 4(a) shows the typical time histories of strain and strain rate of the kidney cortex tissue at a strain rate of $2,000 \text{ s}^{-1}$. The strain-rate history is computed by Equation (1) and the strain history by Equation (2). The nearly flat-top of the strain-rate history curve is an indication that a constant strain rate was achieved during the experiment. The axial force histories on both end-faces of the tissue specimen, as measured by the quartz-crystal force transducers, are shown in Figure 4(b). The overlapped force histories indicate that the specimen deformed under a dynamically equilibrated stress state during the impact loading.

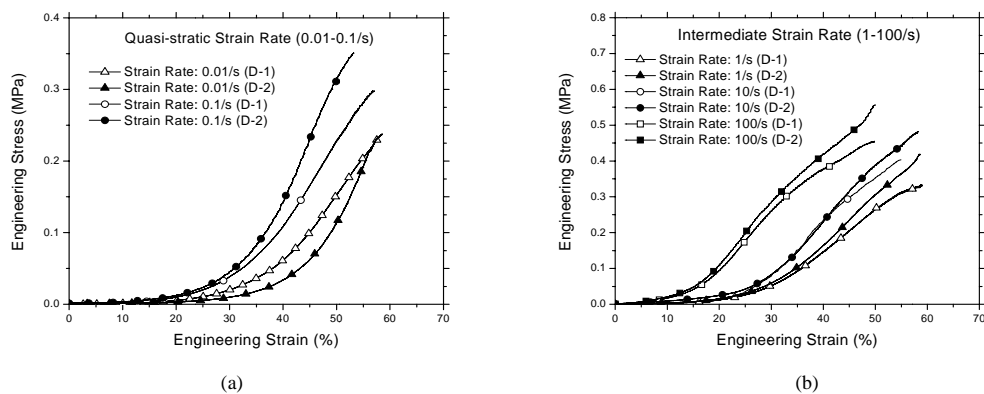


Figure 3: Engineering stress-strain curves of bovine kidney cortex under uniaxial compression at a) quasi-static and b) intermediate strain rates.

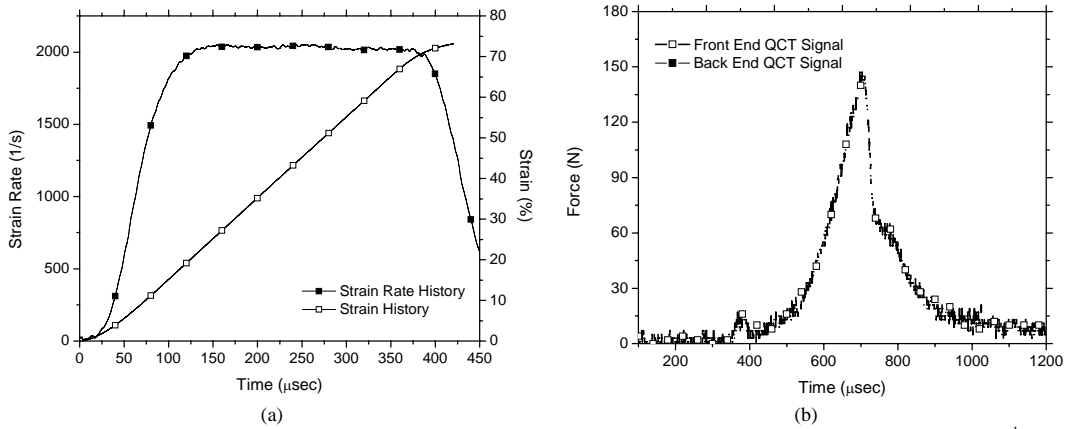


Figure 4: (a) Strain and strain-rate history; (b) Dynamic stress equilibrium of an experiment at the strain rate of $2,000 \text{ s}^{-1}$.

The stress-strain curves obtained from the Kolsky bar experiments are presented in Figure 5. The stress history is computed using Equation (3). These results indicate that the compressive stress-strain behavior strongly depends on strain rates in this range. The kidney tissues become much stiffer when deforming at the strain rates encountered in the Kolsky bar experiments. Figure 5(a) shows five compressive stress-strain curves obtained at the strain rate of $2,000 \text{ s}^{-1}$, which are randomly taken from fifteen experiments. Only five of these are shown for the purpose of clarity. The tight scatter band displayed by these stress-strain curves indicates that the renal cortex is nearly homogeneous in nature as the specimens were taken randomly from different lobes. Figure 5(b) shows the influence of the strain rate on the compressive stress-strain response of the cortex tissue specimens. In this high-rate range, the kidney tissues become stiffer with increasing strain rates. Compared to the stress-strain results obtained at low strain rates at 50% strain, the stress value at $3,000 \text{ s}^{-1}$ strain rate is almost ten times higher than that at 0.01 s^{-1} strain rate and three times higher than that at 100 s^{-1} , as shown in Figure 6. Compared to most engineering materials, such strain-rate effects are drastic. The mechanisms that are responsible for the measured strain-rate effects are not exactly clear. We are interpreting the experimental results as if the tissues were engineering materials. However, the kidney tissues are extremely soft materials with fluid compared to most engineering materials. Other data reductions schemes are possible for such soft materials are under investigation.

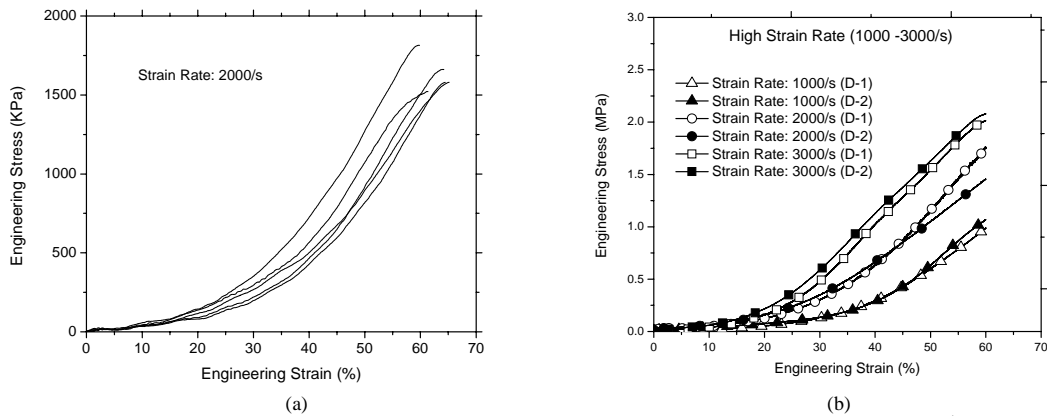


Figure 5: High-rate compressive stress-strain curves (a) showing the extent of repeatability at $2,000 \text{ s}^{-1}$, (b) showing the effect of strain rate and loading direction

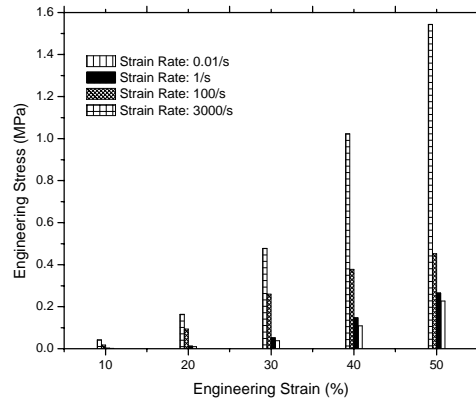


Figure 6: Strain rate effect of renal cortex in D-1 direction

To evaluate the directional anisotropy of the tissues, we conducted compression experiments on specimens taken from both D-1 and D-2 directions at different strain rates. As we can see from the stress-strain curves shown in Figs. 3 and 5(b), the difference between the average stress-strain curves of the kidney cortex tissue loaded along D-1 and D-2 direction at each strain rate appears to be within the error band. This insignificant difference is observed at all the strain rates covered in this study, which indicates that the kidney cortex tissue can be considered nearly isotropic.

5. Conclusions

The compressive stress-strain behavior of steer kidney tissue (cortex) has been experimentally determined at different strain rates ranging from 0.01 s^{-1} to $3,000 \text{ s}^{-1}$. An MTS machine was used to conduct the experiments at quasi-static and intermediate rates, while a modified Kolsky bar was used to perform high-rate experiments. The specimens were harvested from the cortex along two perpendicular directions. The experimental results show that the compressive stress-strain response of the kidney tissue is non-linear and highly strain-rate sensitive. The results from specimens obtained along different directions from different lobes of the tissue indicate that the tissue material is nearly homogeneous and isotropic. The extremely soft tissue specimen exhibits drastic rate effects at strain rates in the Kolsky bar range and may need further examination of other data reduction schemes to explain the reasons behind these observed significant rate effects.

Acknowledgement

This research was supported by a Collaborative Agreement between US Army Research Laboratory and Purdue University. The author would like to acknowledge the Animal Science Department at Purdue University for providing the fresh bovine kidneys.

References

- Beverstock R., Simons R., McLoughlin M., 2001. Severe blunt renal trauma: a 7 year retrospective review from a provincial trauma center. *Can. J. Urol* **8**(5), pp. 1372-1376.
- Casem D., Weerasooriya T. Moy P., 2005. Inertial effects of quartz force transducers embedded in a split Hopkinson pressure bar. *Exp. Mech.* **45**, pp. 368-376.
- Chen, W., Zhang, B. and Forrestal, J., 1999. A split Hopkinson Bar Technique for low-impedance materials, *Exp. Mech.* **39**(2), pp.81-85.
- Chen, W., Lu, F. Zhou B., 2000. A quartz-crystal-embedded Split Hopkinson Pressure bar for soft materials. *Exp. Mech.* **40**(1), pp. 1-6.
- Farshad, M., Barbezat, M., Flueller, P., Schmidlin, F., 1999. Material characterization of the pig kidney in relation with the biomechanical analysis of renal trauma. *J. Biomech.* **32**, pp. 417-425.

- Frew D., Forrestal M., Chen W., 2002. Pulse shaping techniques for testing brittle materials with a split Hopkinson pressure bar. *Exp. Mech.* **42**, pp. 93-106.
- Gary G., 2000. Classic split-Hopkinson pressure bar testing. *Mechanical Testing and Evaluation, Metals Handbook, American Society for Metals* **8**, pp. 462-476.
- Nasseri, S., Bilston, L., Phan-Thein, N., 2002. Viscoelastic properties of pig kidney in shear, experimental results and modeling. *Rheol. Acta.* **41**, pp. 180-192.
- Nava, A., Mazza, E., Kleinerman, F., Avis, N., 2004. Evaluation of the mechanical properties of human liver and kidney through aspiration experiments. *Technol. Health Care* **12**, pp. 269-280.
- Pervin, F., and Chen, W., 2009. Dynamic mechanical response of bovine gray matter and white matter brain tissues under compression. *J. Biomech.* **42**, pp. 731-735.
- Phan-Thein, N. Nasseri, S. Bilston, L., 2000. Oscillatory squeezing flow of a biological material. *Rheol. Acta.* **39**, pp. 409-417.
- Rutledge, R. Thomson, M., Oller, D., 1991. The spectrum of abdominal injuries associated with the use of seat belts. *J. Trauma* **31**, pp. 820-826.
- Schidlin, R., Schid, P., Kurtyka, T., Iselin, C., 1996. Force transmission and stress distribution in a computer-simulated model of the kidney: An analysis of the injury mechanism in renal trauma. *J. Trauma* **40**(5), pp. 791-796.
- Song, B. Chen, W. Ge, Y. Weeresooriya, T., 2007. Dynamic and quasi-static compression response of porcine muscle, *J. Biomech.* **40**, pp. 2999-3005.